International Journal of Scientific Engineering and Applied Science (IJSEAS) – Volume-2, Issue-6,June 2016
ISSN: 2395-3470
www.ijseas.com

Stability regions in controller parameter space of DC motor speed control system with communication delays

Şahin Sönmez, Saffet Ayasun
Department of Electrical and Electronics Engineering, Nigde University, 51240, Nigde, Turkey

Abstract
This paper presents a comprehensive stability analysis of a DC motor speed control system with communication delays. An effective and simple graphical method is proposed to compute all stabilizing Proportional Integral (PI) controller gains of a DC motor speed control system with communication time delay. The approach is based on extracting stability region and the stability boundary locus in the PI controller parameter space having user defined gain and phase margins, and relative stability. The time-domain simulation studies indicate that the proposed schemes give better desired dynamic performance as compared to the recently developed schemes for DC motor speed control with communication delays.
Keywords: *Control Design, Delay Systems, DC Motor Speed Control, Gain and Phase Margins, Stability region.*

1. Introduction

The issue of time delay in feedback control has been received considerable attention in recent years with the proliferation of networked control systems (NCSs) [1-3]. The time delays in NCSs known as network-induced delay consist of sensor-to-controller delay and controller-to-actuator delay. Even though the advances in communication networks have reduced the magnitude of the networked-induced delay significantly, it still cannot be ignored when designing a control system. It is well known that time delays can degrade the performance of control systems and can even make closed-loop system unstable [4-7].

The DC motor control system is a typical example of control systems in which the undesirable impacts of time delays on the system dynamic are observed [3]. DC motor control systems are stable systems in general when time delays are not considered. However, inevitable time delays may destabilize the closed-loop system when the DC motor is controlled through a network. Therefore, communication and measurement delays for stability analysis of a networked-controlled DC motor must be taken into account in the process of a controller design, and methods need to be developed to compute the stability boundaries in terms of time delay and controller parameters. [8-9].

The description of the system stability boundary in terms of time delay for a given set of controller parameters includes the computation of maximum time delays, known as delay margin, such that the system will be stable. On the other hand, one also needs to identify all possible controller parameters, known as stability region, for a given time delay that guaranties a stable operation. Such stability boundaries help us design an appropriate controller for cases in which uncertainty in network-induced delays is unavoidable. To the best of our knowledge, the stability of networked control DC motor speed control systems has not been comprehensively analyzed, and in particular, the description of the stability boundary in terms of the controller parameters for a given time delay has not been reported in the literature.

The existing studies in the stability analysis of time-delayed systems mainly focus on the stability delay margin computation for a given set of controller parameters. Delay margin computation methods could be grouped into two main types, namely frequency-domain direct and time-domain indirect methods. The main goal of frequency domain approaches is to compute all critical purely imaginary roots of the characteristic equation for which the system will be marginally stable. The following three methods are the ones commonly used in delay margin computation: i) Schur-Cohn method [10]; ii) Elimination of exponential terms in the characteristic equation [11]; iii) Rekasius substitution [12]. Among these direct methods, the method based on the

elimination of exponential terms has been implemented into delay margin computation of DC motor speed control system with constant communication delay [13]. The indirect time-domain methods that utilize Lyapunov stability theory and linear matrix inequalities (LMIs) techniques have been used to estimate delay margins of the time-delayed dynamical systems with a PI controller [14-15].

Both frequency and time-domain methods discussed above aim to compute delay margins for a given set of PI controllers. However, for a complete picture of the stability of DC motor control system, it is also essential to determine all possible values of PI controller parameters that ensure a stable operation when a certain amount of time delay is observed in the system. Because, in practical networked-controlled systems, the maximum value of time delays that might be observed is known and on needs to determine the set of PI controller parameters that makes the closed-loop system stable. In one of our earlier work [16], a graphical method based on stability boundary [17-18] has been applied to stability analysis of time-delayed load frequency control systems, and a stability region for a given time delay has been determined in the PI controller parameters space, (K_I, K_P)-plane. However, for the analysis and design of practical control systems, besides stability feature, gain margin (GM) and phase margin (PM) are two important design specifications that must be taken into account in computing stability regions [19]. A set of PI controller parameters that guarantees not only the stability but also desired gain-phase margins of the time-delayed DC motor speed control system must be determined. For that purpose, the time-delayed DC motor speed control system [13] is modified to include a frequency independent Gain Phase Margin Tester (GPMT) as a "virtual compensator" in the feedforward part of the DC motor speed control system model.

This paper extends our earlier work [13] to compute all stabilizing PI controller parameters that ensure a desired dynamic performance of time-delayed DC motor speed control system with user defined phase-gain margins. The approach is based on the stability boundary locus, which can be easily obtained by equating the real and imaginary parts of the characteristic equation to zero. The proposed method has been effectively applied to controller design and synthesis of time-delayed integrating systems [20] and large wind turbine systems [21]. The impact of the user-defined phase and gain margins on the stability region is analyzed. It has been observed that the stability region becomes smaller as the gain and phase margins increase.

In addition to gain-phase margins specifications, in the analysis and design of control systems, it is also important to shift all poles of the characteristic equation of control system to a desired region in the complex plane, for example, to a shifted half plane that guarantees a specific settling time of the system response. In this paper, a relative stability region (K_I, K_P)-plane is also determined. All values of (K_I, K_P) will put all the closed loop poles to the left of a desired $s = \sigma$ (σ is constant). Finally, the accuracy and effectiveness of the proposed methods are also verified by using time-domain simulation capabilities of Matlab/Simulink [22].

2. Modified DC Motor System Model With GPMT

The block diagram of a DC motor system with a communication delay into the control loop is shown in Figure 1. The dynamic of a DC motor driving a load is described by a differential equation of the mechanical system and volt-ampere equations of the armature circuit [3], [6].

$$J\frac{d\omega_m}{dt} + B\omega_m + T_l = T_e = Ki_a$$
$$u(t) = v_a = e_a + R_a i_a + L_a\, di_a/dt \qquad (1)$$

where $u = v_a$ is the armature winding input voltage, i_a, R_a and L_a are the current, resistance, and inductance of the armature circuit; respectively; $e_a = K_a\omega_m$ is the back-electromotive-force (EMF) voltage (i.e., generated speed voltage); ω_m is the angular speed of the motor; T_e and T_l are the electromagnetic torque developed by the motor and the mechanical load torque opposing direction; J is the combined moment of inertia of the load and the rotor, B is the equivalent viscous friction constant of

the load and the motor; K and K_a are the torque constant and the back-EMF constant, respectively. The transfer function of the DC motor could be easily obtained as

$$G(s) = \frac{\frac{K}{JL_a}}{s^2 + \left(\frac{R_a}{L_a} + \frac{B}{J}\right)s + \frac{R_aB + KK_a}{JL}}. \qquad (2)$$

The transfer function of proportional-integral (PI) controller is given as follows:

$$G_c(s) = K_P + \frac{K_I}{s} \qquad (3)$$

where K_P and K_I are the proportional and integral gains, respectively. The proportional term affects the rate of angular speed rise after a step change. The integral term affects the angular speed settling time after initial overshoot. The integral controller adds a pole at origin and increases the system type by one and reduces the steady-state error. The combined effect of the PI controller will shape the response of the speed control system to reach the desired performance.

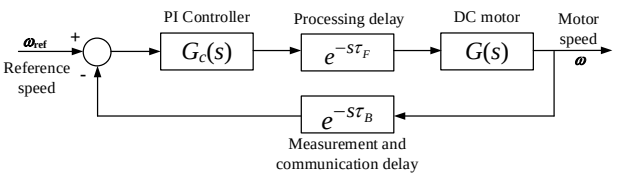

Fig. 1. Block diagram of a DC motor control system with time delays.

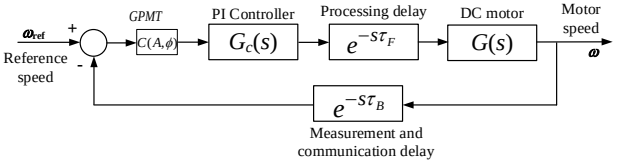

Fig. 2. Modified block diagram of a DC motor control system with a GPMT.

As illustrated in Figure 1, all time delays in the feedback loop that are lumped together into a feedback delay (τ_B) between the output and the controller. This delay represents the measurement and communication delays (sensor-to-controller delay). The controller processing and communication delay (τ_F) (controller-to-actuator delay) is placed in the feedforward part between the controller and DC motor. For the stability analysis, the characteristic equation given below of DC motor control system with time delay is required [13].

$$\Delta(s,\tau) = P(s) + Q(s)e^{-s\tau} = 0 \qquad (4)$$

where $\tau = \tau_B + \tau_F$ is the total time delay. $P(s)$, $Q(s)$ are polynomials in s with real coefficients given in Eq. (2).

$$\Delta(s,\tau) = p_3s^3 + p_2s^2 + p_1s + (q_1s + q_0)e^{-s\tau} = 0$$
$$p_3 = 1, p_2 = \frac{R_a}{L_a} + \frac{B}{J}, p_1 = \frac{R_aB + KK_a}{JL_a}$$
$$q_1 = \frac{KK_P}{JL_a}, q_0 = \frac{KK_I}{JL_a} \qquad (5)$$

The user defined gain and phase margins tester (GPMT) as a “virtual compensator” is added to the feedforward path in control loop of the DC motor system as shown in Figure 2. The frequency independent GPMT is given in the form:

$$C(A,\phi) = Ae^{-j\phi} \qquad (6)$$

where A and ϕ represent gain and phase margins, respectively.

To find the controller parameters for a given value of gain margin A of the DC motor speed control system given in Figure 2, one needs to set $\phi = 0$ in Eq. (6). On the other hand, setting $A = 1$ in Eq. (6), one can obtain the controller parameters for a given phase margin ϕ. The characteristic equation of the DC motor speed control system with a GPMT given in Figure 2 is first obtained.

$$\Delta(s,\tau') = P'(s) + Q'(s)e^{-s\tau}e^{-j\phi} = 0$$
$$= P'(s) + Q'(s)e^{-s\tau'} = 0 \qquad (7)$$

Where

$$P'(s) = P(s) = p_3 s^3 + p_2 s^2 + p_1 s$$
$$Q'(s) = A\left(KK_P / JL_a\right)s + A\left(KK_I / JL_a\right) = q_1' s + q_0'$$

Note that in Eq. (7) we have an exponential term $e^{-s\tau'}$ rather than $e^{-s\tau}$ as in Eq. (1). This is obtained by combining $e^{-s\tau}$ and $e^{-j\phi}$ into a single exponential terms for $s = j\omega_c$ which is the root of Eq. (7) on the imaginary axis. The relationship between and is given as

$$\tau' = \tau + \frac{\phi}{\omega_c} \qquad (8)$$

3. Gain and Phase Margins Based Stability Region

In order to obtain the boundary of the stability region, we substitute $s = j\omega_c$ and $\omega_c > 0$ into the characteristic equation in Eq. (7) as follows

$$\Delta(j\omega_c, \tau') = A\left(K/JL_a\right)e^{-j\omega_c\tau'}\left(K_P(j\omega_c) + K_I\right) + p_3(j\omega_c)^3 + p_2(j\omega_c)^2 + p_1(j\omega_c) = 0 \qquad (9)$$

Substituting $e^{-j\omega\tau'} = \cos(\omega\tau') - j\sin(\omega\tau')$ into Eq. (9) and separating into the real and imaginary parts, we obtain the following characteristic equation.

$$\Delta(j\omega, \tau') = \left[A\left(K/JL_a\right)\omega_c \sin(\omega_c\tau')\right]K_P + \left[A\left(K/JL_a\right)\cos(\omega_c\tau')\right]K_I - p_2{\omega_c}^2 + j\left(\left[A\left(K/JL_a\right)\omega_c \cos(\omega_c\tau')\right]K_P + \left[-A\left(K/JL_a\right)\sin(\omega_c\tau')\right]K_I - p_3{\omega_c}^3 + p_1\omega_c\right) = 0 \qquad (10)$$

Equating the real and imaginary parts of $\Delta(j\omega_c, \tau')$ in Eq. (10) to zero, we get the following equations.

$$K_P A_1(\omega_c) + K_I B_1(\omega_c) + C_1(\omega_c) = 0$$
$$K_P A_2(\omega_c) + K_I B_2(\omega_c) + C_2(\omega_c) = 0 \qquad (11)$$

where

$$A_1(\omega_c) = A\left(K/JL_a\right)\omega_c \sin(\omega_c\tau');$$
$$B_1(\omega_c) = A\left(K/JL_a\right)\cos(\omega_c\tau');\ C_1(\omega_c) = -p_2{\omega_c}^2;$$
$$A_2(\omega_c) = A\left(K/JL_a\right)\omega_c \cos(\omega_c\tau');$$
$$B_2(\omega_c) = -A\left(K/JL_a\right)\sin(\omega_c\tau');$$
$$C_2(\omega_c) = -p_3{\omega_c}^3 + p_1\omega_c$$

Solving two equations in Eq. (11) simultaneously, the stability boundary locus $\ell(K_P, K_I, \omega_c)$ in the (K_I, K_P)-plane is obtained.

$$K_P = \frac{B_1(\omega_c)C_2(\omega_c) - B_2(\omega_c)C_1(\omega_c)}{A_1(\omega_c)B_2(\omega_c) - A_2(\omega_c)B_1(\omega_c)}$$
$$K_I = \frac{A_2(\omega)C_1(\omega) - A_1(\omega)C_2(\omega)}{A_1(\omega_c)B_2(\omega_c) - A_2(\omega_c)B_1(\omega_c)} \qquad (12)$$

Note that the line $K_I = 0$ is also in the boundary locus since a real root of $\Delta(s, \tau') = 0$ given in Eq. (9) can cross the imaginary axis at $s = j\omega_c = 0$ for $K_I = 0$. Therefore, the stability boundary locus, $\ell(K_P, K_I, \omega_c)$ and the line $K_I = 0$ divide (K_I, K_P)-plane into stable and unstable regions. This part of the boundary locus is known as the Real Root Boundary (RRB) and the one obtained from Eq. (12) is defined as the Complex Root Boundary (CRB) of the stability region [17-18].

4. Relative Stability Region

In this section, the graphical approach is further developed to obtain relative stability regions. In the analysis and design of control systems, it is important to shift all poles of the characteristic equation of time-delayed DC motor control system to a desired region in the complex plane, for example, to a shifted half plane that guarantees a specific settling time of the system speed response. The objective of this section is to compute all values of (K_I, K_P) that will put all the closed loop poles to the left of a desired $s = \sigma$ (σ is negative constant). Using $s + \sigma$ instead of s in Equations (4)-(5) we obtain the corresponding characteristic equation as

$$\Delta(s+\sigma,\tau) = P(s+\sigma) + Q(s+\sigma)e^{-\tau(s+\sigma)} = 0$$
$$\Delta(s+\sigma,\tau) = p_3(s+\sigma)^3 + p_2(s+\sigma)^2 + p_1(s+\sigma)$$
$$+\left(K/JL_a\right)e^{-(s+\sigma)\tau}\left(K_P(s+\sigma)+K_I\right) = 0 \quad (13)$$

First we substitute $s = j\omega_c$ with $\omega_c > 0$ and $e^{-(j\omega_c+\sigma)\tau} = e^{-\sigma\tau}\left[\cos(\omega_c\tau) - j\sin(\omega_c\tau)\right]$ into Eq. (13) and equate its real and imaginary parts into zero to determine the following equations.

$$K_P A_1(\omega_c) + K_I B_1(\omega_c) + C_1(\omega_c) = 0$$
$$K_P A_2(\omega_c) + K_I B_2(\omega_c) + C_2(\omega_c) = 0 \quad (14)$$

where

$$A_1(\omega_c) = \left(K/JL_a\right)\left(\mathrm{e}^{-\sigma\tau}\,\sigma\cos(\omega_c\tau) + \mathrm{e}^{-\sigma\tau}\,\omega_c\sin(\omega_c\tau)\right);$$
$$B_1(\omega_c) = \left(K/JL_a\right)\mathrm{e}^{-\sigma\tau}\cos(\omega_c\tau);$$
$$C_1(\omega_c) = -{\omega_c}^2\left(3\sigma p_3 + p_2\right) + \left(p_1\sigma + p_2\sigma^2 + p_3\sigma^3\right);$$
$$A_2(\omega) = \left(K/JL_a\right)\left(\mathrm{e}^{-\sigma\tau}\,\omega_c\cos(\omega_c\tau) - \mathrm{e}^{-\sigma\tau}\,\sigma\sin(\omega_c\tau)\right);$$
$$B_2(\omega_c) = -\left(K/JL_a\right)\mathrm{e}^{-\sigma\tau}\sin(\omega_c\tau);$$
$$C_2(\omega_c) = -p_3{\omega_c}^3 + \omega_c\left(p_1 + 2p_2\sigma + 3p_3\sigma^2\right) \quad (15)$$

Solving two equations in Eq. (14) simultaneously, the stability boundary locus $\ell(K_P, K_I, \omega_c)$ in the (K_I, K_P)-plane is obtained as:

$$K_P = \frac{B_1(\omega_c)C_2(\omega_c) - B_2(\omega_c)C_1(\omega_c)}{A_1(\omega_c)B_2(\omega_c) - A_2(\omega_c)B_1(\omega_c)}$$
$$K_I = \frac{A_2(\omega_c)C_1(\omega_c) - A_1(\omega_c)C_2(\omega_c)}{A_1(\omega_c)B_2(\omega_c) - A_2(\omega_c)B_1(\omega_c)} \quad (16)$$

Similar to the previous section, we need to set $s = j\omega_c = 0$ to determine the real root boundary. It is clear from Equations (14)-(15) that A_2, B_2, C_2 become all zero for $s = j\omega_c = 0$. Then, the functional relation between K_I and K_P could be easily determined from $K_P A_1(\omega) + K_I B_1(\omega) + C_1(\omega) = 0$ as

$$K_I = -\sigma K_P - \frac{(p_3\sigma^3 + p_2\sigma^2 + p_1\sigma)}{\left(K/JL_a\right)e^{-\sigma\tau}} \quad (17)$$

Note that the real root boundary defined by Eq. (17) is a straight line (K_I, K_P)-plane.

4. Results

The section presents stability regions based on both gain-phase margins, and location of the roots of the characteristic equation. The parameters of the DC motor control system are given in [3] and [13].

4.1 Relative stability regions based on gain and phase margins

The time delay is chosen as $\tau = 0.5s$ and the crossing frequency is selected in the range of $\omega \in [0,10]$ *rad* / *s* for stability boundary locus. Our first main purpose is to determine the stabilizing values of K_P and K_I such that the characteristic equation of Eq. (7) should be Hurwitz stable with desired gain and phase margins. Suppose our desired phase and gain margins are $A \geq 2$ and $\phi \geq 10^0$, respectively, then we substitute $A = 2$ and $\phi = 0^0$ in Equations (10)-(12) and get the stability boundary locus (SBL) for specific gain margin with a crossing frequency of $\omega = 3.908$ *rad* / *s*. The corresponding stability region is labeled as R1 in Figure 3. Similarly, by substituting $A = 1$ and $\phi = 10^0$ in Equations (10)-(12), we obtain the SBL for specific phase margin with a crossing frequency of $\omega = 3.6410$ *rad* / *s*. The stability region is denoted by R2. The intersection of R1 and R2 regions gives the stability region in (K_P, K_I) -plane shown in Figure 3, and ensures the DC motor speed control system will have a desired gain and phase margins of $A \geq 2$ and $\phi \geq 10^0$. Finally, the stability region without considering phase and gain margins is determined by substituting $A = 1$ and $\phi = 0^0$ in Equations (10)-(12). This region is represented by R3 in Figure 3. Observe that stability region with desired gain and/or phase margins, R1 and R2 are much smaller than stability region R3.

Next, we select three points each region, $(K_P = 0.02, K_I = 0.03)$ in R1, $(K_P = 0.02, K_I = 0.06)$ in R2, and $(K_P = 0.02, K_I = 0.085)$ in R3 region, respectively. Figure 4 shows the speed responses of the DC motor control system. It is clear that all responses are stable. However, the speed deviation for $(K_P = 0.02, K_I = 0.085)$ contain undesirable oscillations as compared to other two responses. From a practical point of view, such oscillations are not acceptable. It is clear that the disturbance rejection performance of the DC motor speed control system is quicker and non-oscillatory for the (K_P, K_I) values selected from relative stability regions R1 and R2 with desired gain and/or phase margins.

Moreover, the impact of the time delay on the size and shape of the stability region for a given gain-and phase margin is investigated. Figure 5 shows stability regions for three different time delays, $\tau = 0.5\ s, \tau = 1.0\ s, \tau = 1.5\ s$ and $A = 2, \phi = 0^0$. It is clear that the size stability region decreases and the shape does not change as the time delay increases.

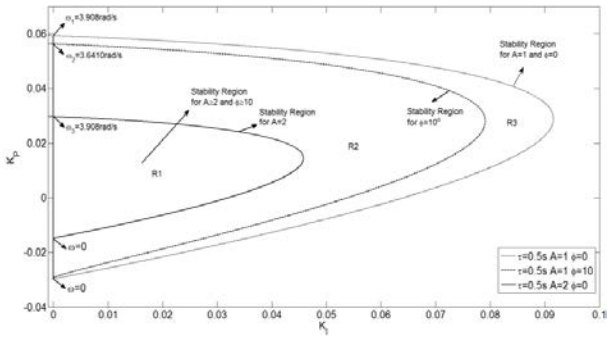

Fig. 3. Stability region of PI controller for $A \geq 2$, $\phi \geq 10^0$, and $\tau = 0.5\ s$.

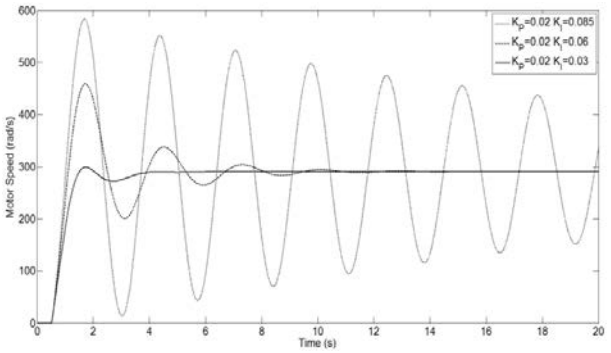

Fig. 4. Speed deviation responses for three different values controller gains.

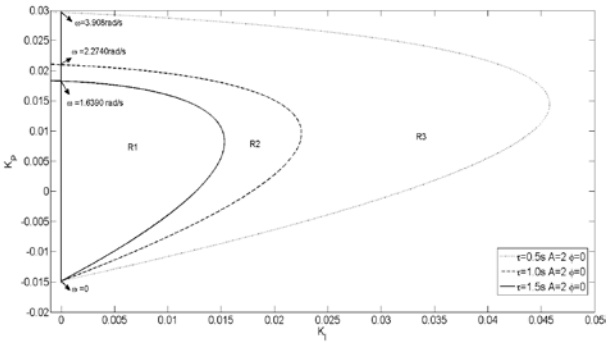

Fig. 5. Stability region of PI controller for three different time delays and $A = 2, \phi = 0$.

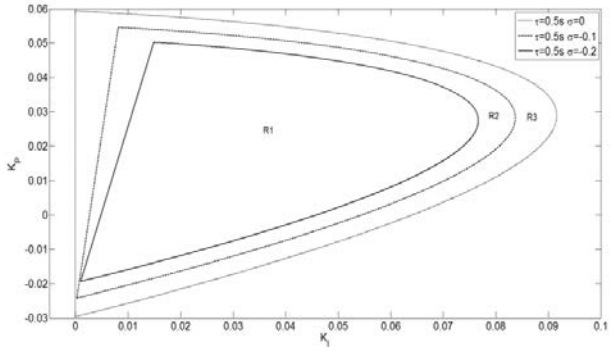

Fig. 6. Relative stability regions for $\sigma = 0, -0.1, -0.2$.

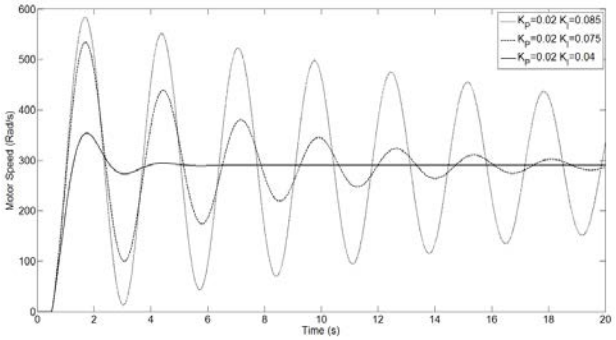

Fig. 7. Speed deviation responses for three different values controller gains.

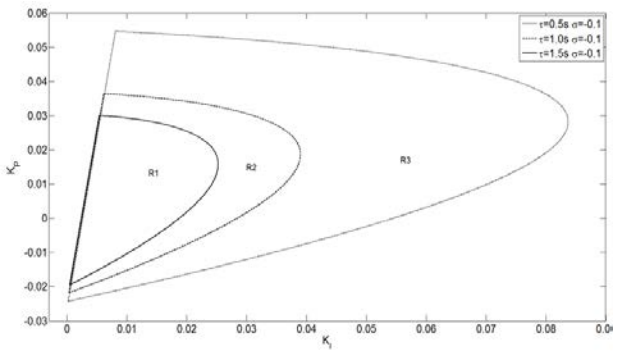

Fig. 8. Relative stability regions for three different time delays and $\sigma = -0.1$.

4.2 Relative stability regions based on the root location

Our second main purpose is to obtain all stabilizing values of K_P and K_I such that the characteristic equation of Eq. (13) should be Hurwitz stable and its roots should lie in a desired region with a boundary $s = \sigma \ \ (\sigma < 0)$ in the left-half complex plane. Similar procedure of the gain-phase margins case is followed and relative stability regions are obtained for three different σ values, $\sigma = 0$, $\sigma = -0.1$ and $\sigma = -0.2$. Figure 6 presents the corresponding relative stability regions for $\tau = 0.5s$. Note that the region for $\sigma = 0$ is the same region R3 in Figure 3, whose stability boundary is the imaginary axis. Note that R1 region with $\sigma = -0.2$ and R2 region with $\sigma = -0.1$ are much smaller that R3 region with $\sigma = 0$ as expected. The complex root boundary of R1 and R2 are determined by Eq. (16) while the real root boundary of R3 is determined by Eq. (17). Time-domain simulations are carried out for three different (K_P, K_I) values one each region, $(K_P = 0.02, K_I = 0.04)$ in R1, $(K_P = 0.02, K_I = 0.075)$ in R2 and $(K_P = 0.02, K_I = 0.085)$ in R3. Figure 7 depicts the speed deviations of the time-delayed DC motor control system. Once again, the controller gains chosen from R1 gives better dynamic performance without having any oscillations in the speed deviation and the speed deviation quickly reaches to zero.

Additionally, the effect of the time delay on the relative stability region is the same as the gain-phase based stability regions. Figure 8 illustrates how the size of the region decreases as the time delay increases for $\sigma = -0.1$.

4. Conclusions

This paper has presented a graphical method based on the stability boundary locus to determine stability regions in the PI controller parameter space for user defined gain-phase margins and for a desired location of the closed-loop roots of DC motor speed control system with communication delay. The relative stability regions provide us all stabilizing values of controller gains that ensure that the time-delayed DC motor speed control system will have desired gain and phase margins. Relative stability regions shrink as gain and/or phase margins increase.

With the help of the stability region, the PI controller parameters could be properly selected such that the DC motor speed control containing certain amount of communication delay will be not only stable and but also will have a desired dynamic performance in terms of damping, settling time and non-oscillatory behaviors.

References

[1] P. Antsaklis, and J. Baillieul, “Special issue on networked control systems”, IEEE Transactions on Automatic Control, Vol. 49, No. 9, 2004, pp. 1421-1597.

[2] W. Zhang, M.S. Branicky, and S.M. Phillips, “Stability of networked control systems”, IEEE Control System Magazine, Vol. 21, No. 1, 2001, pp. 84-99.

[3] M.Y. Chow, and Y. Tipsuwan, “Gain adaptation of networked DC motor controllers based on QOS variations”, IEEE Transactions on Industrial Electronics, Vol. 50, No. 5, 2003, pp. 936-943.

[4] D.S. Kim, Y.S. Lee, W.H. Kwon, and H.S. Park, “Maximum allowable delay bounds of networked control systems”, Control Engineering Practice, Vol. 11, No. 1, 2003, pp. 1301-1313.

[5] C. Tan, L. Li, H. Zhang, “Stabilization of networked control systems with both network-induced delay and packet dropout”, Automatica, Vol. 59, 2015, pp. 194-199.

[6] Y. Tipsuwan, and M.Y. Chow, "Gain scheduler middleware: A methodology to enable existing controllers for networked control and teleoperation—part I: networked control", IEEE Transactions on Industrial Electronics, Vol. 51, No. 6, 2004, pp. 1218-1227.
[7] Y. Tipsuwan, and M.Y. Chow, "On the gain scheduling for networked PI controller over IP network", IEEE/ASME Transactions on Mechatronics, Vol. 9, No. 3, 2004, pp. 491-498.
[8] Z. Li, Bai, Y. Huang, and Y. Cai "Novel delay-partitioning stabilization approach for networked control system via Wirtinger-based inequalities", ISA Transactions, Vol. 61, 2016, pp. 75-86.
[9] K. Li, and R. Bhattacharya, "Stability analysis of large-scale distributed networked control systems with random communication delays: A switched system approach", System & Control Letters, Vol. 85, 2015, pp. 77-83.
[10] J. Chen, G. Gu, and C.N. Nett, "A new method for computing delay margins for stability of linear delay systems", System and Control Letters, Vol. 26, No. 2, 1995, pp. 107-117.
[11] K.E. Walton, and J.E. Marshall, J.E. "Direct method for TDS stability analysis", IEE Proceeding Part D, Vol. 134, No. 2, 1987, pp. 101–107.
[12] N. Olgac, and R. Sipahi, "An exact method for the stability analysis of time-delayed linear time-invariant (LTI) systems", IEEE Transactions on Automatic Control, Vol. 47, No. 5, 2002, pp. 793-797.
[13] S. Ayasun, "Stability analysis of time-delayed DC motor speed control system", Turkish Journal of Electrical Engineering & Computer Sciences, Vol. 21, No. 2, 2013, pp. 381-393.
[14] M. Liu, L. Yang, D. Gan, D. Wang, F. Gao, and Y. Chen, "The stability of AGC systems with commensurate delays", European Transactions on Electrical Power, Vol. 17, No. 6, 2007, pp. 615-627.
[15] L. Jiang, W. Yao, Q.H. Wu, J.Y. Wen, and S.J. Cheng, "Delay-dependent stability for load frequency control with constant and time-varying delays", IEEE Transactions on Power Systems, Vol. 27, No. 2, 2012, pp. 932-941.
[16] Ş. Sönmez, and S, Ayasun, "Stability region in the parameter space of PI controller for a single-area load frequency control system with time delay", IEEE Transactions on Power Systems, Vol. 31, No. 1, 2016, pp. 370-377.
[17] M.T. Söylemez, N. Munro, H. Baki, "Fast calculation of stabilizing PID controller", Automatica, Vol. 39, No. 1, 2003, pp. 121–126.
[18] N. Tan, I. Kaya, C. Yeroglu, and D.P. Atherton, "Computation of stabilizing PI and PID controllers using the stability boundary locus", Energy Conversion and Management, Vol. 47, No. 18-19, 2006, pp. 3045-3058.
[19] C.H. Chang, and K.W. Han, "Gain margins and phase margins for control systems with adjustable parameters", Journal of Guidance Control and Dynamics, Vol. 13, No. 3, 1990, pp. 404-408.
[20] S.E. Hamamcı, and M. Köksal, "Calculation of all stabilizing fractional-order PD controllers for integrating time delays", Computers and Mathematics with Applications, Vol. 59, No. 5, 2010, pp. 1621-1629.
[21] J. Wang, N. Tse, and Z. Gao, "Synthesis on-PI-based pitch controller of large wind turbine generator", Energy Conversion and Management, Vol. 52, No. 2, 2011, pp. 1288-1294.
[22] Simulink, Model-Based and System-Based Design, Using Simulink. MathWorks Inc., Natick, MA, 2000.

Şahin Sönmez is currently working as a research assistant in the Department of Electrical and Electronics Engineering of Nigde University, Turkey. His research interests include modeling and stability analysis of power systems.

Saffet Ayasun is currently working as a professor in the Department of Electrical Engineering of Nigde University, Turkey. His research interests include stability analysis of time delayed dynamical systems and its application into power systems stability analysis.